JOURNAL OF PROPULSION AND POWER
Vol. 15, No. 6, November–December 1999

Linear Stability and Pressure-Driven Response Function of Solid Propellants with Phase Transition

F. Cozzi* and L. T. DeLuca†
Politecnico di Milano, 20133 Milan, Italy
and
B. V. Novozhilov‡
Russian Academy of Sciences, 117977, Moscow, Russia

An extension of the Zel'dovich–Novozhilov approach to adiabatic burning of solid energetic materials subjected to a concentrated phase transition is presented. The pressure-driven frequency response function and intrinsic stability boundary are obtained in the linear approximation of the problem. The intrinsic stability boundary is portrayed as a parametric representation of oscillatory burning frequency. The corresponding previous results are recovered as a special case for no phase transition. The surface-temperature sensitivity parameter *r* is deduced by assuming the Arrhenius surface pyrolysis law. It is shown that phase transition may strongly affect the frequency response function, notwithstanding its limited thermal effect, if the operating point moves closer to the stability boundary. Some typical results are discussed. To validate these theoretical expectations, accurate error estimates of experimental results are needed.

Nomenclature

A	= nondimensional function used in linear frequency response analysis, Eq. (19)
A_1, A_2, A_3	= coefficients used in stability matrix; Sec. III.C
$\tilde{A}_s$	= multiplicative factor of Arrhenius pyrolysis, (cm/s)/(atm)^{n_s}, Eq. (21)
a	= flame modeling (FM) nondimensional stability parameter, Eq. (8)
B	= nondimensional function used in linear frequency response analysis, Eq. (15)
b	= FM nondimensional stability parameter, Eq. (9)
C_1, C_2, C_3, C_4	= constants used in the unsteady condensed phase thermal profiles; Sec. III.B
c	= specific heat, cal/g K
$\tilde{E}$	= activation energy, cal/mol
f	= thermal gradient at condensed-phase side of burning surface, K/cm
i	= imaginary unit
k	= Zel'dovich–Novozhilov (ZN) initial-temperature steady sensitivity parameter, nondimensional, defined in Eq. (3)
$k_{(\ldots)}$	= thermal conductivity, cal/cm · s · K
ℓ_{tra}	= transition position, cm
m	= mass burning rate, g/cm^2 · s
n	= pressure exponent of ballistic steady burning rate, nondimensional, Eq. (17)
n_s	= pressure exponent of pyrolysis law, nondimensional, Eq. (21) (Arrhenius)
n_{T_s}	= pressure sensitivity of steady surface temperature, nondimensional, Eq. (20)
p	= pressure, atm
p_{ref}	= reference pressure (68 atm)
Q	= heat release, cal/g (positive if exothermic)
R_p	= mass burning rate response to pressure fluctuations, defined in Eq. (85)
$\Re$	= universal gas constant, 1.987 cal/mol · K
r	= ZN initial-temperature steady sensitivity parameter, nondimensional, defined in Eq. (4)
r_b	= burning rate, cm/s
T	= temperature, K
T_0	= initial propellant temperature, K
t	= time coordinate, s
x	= space coordinate, cm
Z, Z_k, Z_r	= coefficients used in Sec. III.C
$z_{1,2}$	= $[1 \pm \sqrt{(1+4i\Omega)}]/2$, complex characteristic roots of fluctuating thermal profile; Eq. (57)
α	= thermal diffusivity, cm^2/s; condensed-phase parameter defined in Eq. (40)
β	= condensed-phase parameter defined in Eq. (41)
γ	= condensed-phase parameter defined in Eq. (42)
Δ	= condensed-phase parameter defined in Eq. (43)
δ	= ZN Jacobian, nondimensional, defined in Eq. (5)
μ	= ZN pressure sensitivity of steady surface temperature, nondimensional, defined in Eq. (2)
ν	= ZN pressure sensitivity of steady burning rate, nondimensional, defined in Eq. (1)
ρ	= density, g/cm^3
σ_p	= $[\partial \ln \bar{m}/\partial T_0]_{p=\mathrm{const}}$, temperature sensitivity of steady burning rate, 1/K
σ_{T_s}	= $[\partial \ln \bar{T}_s/\partial T_0]_{p=\mathrm{const}}$, temperature sensitivity of steady surface temperature, 1/K
Ω	= nondimensional circular frequency, $\omega \cdot \alpha_c/\bar{r}_b^2$
ω	= circular frequency, rad/s

Subscripts

bif	= bifurcation
c	= condensed phase
i	= initial
im	= imaginary part
p	= pressure
real	= real part
ref	= reference
s	= burning surface
tra	= transition

Received 4 February 1998; revision received 7 August 1998; accepted for publication 10 August 1998.

*Ph.D. Candidate; currently Researcher, Dipartimento di Energetica, 32 Piazza Leonardo da Vinci.

†Professor, Dipartimento di Energetica, 32 Piazza Leonardo da Vinci; DeLuca@icil64.cilea.it. Associate Fellow AIAA.

‡Professor, Institute of Chemical Physics.

Superscripts

$\overline{(\ldots)}$ = steady-state value
$\widetilde{(\ldots)}$ = dimensional value
$()'$ = fluctuating value
$()^*$ = complex conjugate value

I. Introduction

THE current intrinsic stability analyses of solid energetic materials assume chemical reactions concentrated at the burning surface (assumed infinitely thin), and no other chemical activity whatsoever in the condensed phase. However, comparison with experimental results shows discrepancies from the theoretical expectations (e.g., see Ref. 1). Although other factors also may play a role, as a first step to bridge this possible gap an extension of the theory is presented to include concentrated phase transitions somewhere in depth in the condensed phase. Moreover, in several instances, phase transitions—solid to solid or solid to liquid—are known to occur in practical applications. This may affect components of energetic materials, for example, ammonium nitrate (AN)[2,3]; ammonium perchlorate (AP),[4,5] cyclotetramethylenetetranitramine (Ref. 6, p. 142, and Ref. 7, p. 203), cyclotrimethylenetrinitramine (RDX; Ref. 6, p. 142, Ref. 7, p. 203, and Ref. 8); additives to energetic materials, e.g., KCl and LiF (Ref. 9); or just the overall mixture making the energetic material, e.g., AN-based energetic compositions,[10] RDX-based composite propellants,[11] the foam zone in double-base propellants,[12] and so on. The modification of condensed-phase steady thermal profiles due to AP phase transition is clearly shown in Figs. 7–9 of Ref. 13. The extension is conducted within the Zel'dovich–Novozhilov (ZN) framework, but connections with the corresponding flame modeling (FM) framework also are discussed. Both approaches, ZN and FM, share the basic assumptions of quasi-steady gas-phase, homogeneous condensed-phase, and one-dimensional (QSHOD) burning-strand framework. The intrinsic stability boundary of QSHOD burning was found first by Zel'dovich[14,15] in his pioneering work started in 1942, but assuming variable burning rate with a constant surface temperature. This assumption was relaxed in the successive investigations. Novozhilov (e.g.; Refs. 16–19) in 1965 first obtained the QSHOD ZN stability boundary and frequency response function including both variable burning rate and surface temperature.

The corresponding QSHOD FM result for a premixed flame had been obtained previously by Denison and Baum[20] in 1961. A successive investigation conducted by Krier et al.[21] (KTSS) at Princeton University in 1968 extended the FM approach to diffusive flames. Systematic investigations were carried out by Culick for a variety of flame configurations, e.g., Refs. 22–24. All of these investigations were conducted for the linear approximation of pressure-driven burning; in general, except the chemical reactions concentrated at the burning surface, a chemically inert condensed phase was otherwise assumed.

Few papers allowed for chemical reactions distributed in the condensed phase: Results were presented in Refs. 22, 25–30 for pressure-driven burning examined by a variety of techniques. A further generalization of the FM approach was carried out in 1995 1) for the full nonlinear problem with arbitrary flames but limited to chemically inert condensed phase, except the chemical reactions concentrated at the burning surface, and 2) for the linear approximation of the problem but considering also distributed chemical reactions.[31]

The objective of this paper is to determine the intrinsic stability boundary and frequency response function, including in-depth phase transition effects, for the linear approximation of pressure-driven burning, within the ZN framework. Adiabatic burning is assumed.

The problem is formulated in Sec. III. The solution obtained with phase transition is discussed in Sec. III.C (intrinsic stability) and Sec. III.D (frequency response function); the standard solution with no phase transition, recalled in Sec. II, is recovered as a particular case. Typical results are illustrated for the test case shown in Table 1. Conclusions and future work are discussed in Sec. V.

Table 1 Properties of test-case baseline and modifications

Assumed or measured properties
Transition temperature, $T_{\mathrm{tra}} = 513$ K
Transition heat, $Q_{\mathrm{tra}} = -18.3$ cal/g
Initial temperature of sample, $T_0 = 298$ K
Condensed-phase specific heat, $c_c = 0.33$ cal/g K
Burning-rate initial-temperature sensitivity, $\sigma_p = 0.003\ \mathrm{K}^{-1}$
Condensed-phase thermal diffusivity, $\alpha_c = 0.0018\ \mathrm{cm/s}^2$
Steady burning rate, $\bar{r}_b = 1.132 \cdot (\bar{p}/p_{\mathrm{ref}})^{0.526}$ cm/s
Steady burning surface temperature, $\bar{T}_s = 947 \cdot (\bar{p}/p_{\mathrm{ref}})^{0.045}$ k
Surface Arrhenius activation energy, $\tilde{E}_s = 16{,}000$ cal/mol
Pyrolysis law pressure power
(Arrhenius simple), $n_s = 0$
(Arrhenius generalized), $n_s = 0.526 - 0.045 * (16{,}000/1.987 * 947) * (\bar{p}/p_{\mathrm{ref}})^{-0.045}$
Condensed-phase parameter $\gamma \equiv \beta/\alpha = -[c_c(T_{\mathrm{tra}} - T_0)/Q_{\mathrm{tra}}] = 3.877$
Operating pressure, $p = 10$ atm
Modified test-case baseline
Operating pressure, $p = 1$ or 68 atm
Burning-rate initial-temperature sensitivity, $\sigma_p = 0.002$ or $0.004\ \mathrm{K}^{-1}$
Transition temperature, $T_{\mathrm{tra}} = 400$ or 600 K
Transition heat, $Q_{\mathrm{tra}} = -80$ or $+40$ cal/g

II. Standard Solution

In the standard ZN formulation proposed by Novozhilov[16–19] in 1965, four nondimensional steady-state parameters are introduced to describe the dependence of ballistic properties on pressure and ambient temperature

$$\nu \equiv \left[\frac{\partial \ln \bar{m}}{\partial \ln \bar{p}}\right]_{T_0 = \mathrm{const}} \tag{1}$$

$$\mu \equiv \frac{1}{(\bar{T}_s - T_0)}\left[\frac{\partial \bar{T}_s}{\partial \ln \bar{p}}\right]_{T_0 = \mathrm{const}} \tag{2}$$

$$k \equiv (\bar{T}_s - T_0)\left[\frac{\partial \ln \bar{m}}{\partial T_0}\right]_{\bar{p} = \mathrm{const}} \tag{3}$$

$$r \equiv \left[\frac{\partial \bar{T}_s}{\partial T_0}\right]_{\bar{p} = \mathrm{const}} \tag{4}$$

where $\bar{m}_s = \rho_c \bar{r}_b = \bar{m}$ is the steady surface mass burning rate. A possible correlation among the four sensitivity parameters is revealed by the pressure Jacobian defined as

$$\delta \equiv \frac{\partial(\ln \bar{m}, \bar{T}_s)}{\partial(\ln \bar{p}, T_0)} = \nu r - \mu k \tag{5}$$

Should $\delta = 0$, then one of the four sensitivity parameters can be evaluated from the remaining three. A finite value of the Jacobian, although suspected for different compositions, cannot be shown experimentally in a convincing way (e.g., see Ref. 18, pp. 21–22, Ref. 19, pp. 617–618) because of inherent difficulties in measuring surface temperatures even under steady conditions.[32] At any rate, for ZN, one finds in general that

$$\frac{\delta}{r} \equiv \frac{\partial(\ln \bar{m}, \bar{T}_s)/\partial(\ln \bar{p}, T_0)}{[\partial \bar{T}_s/\partial T_0]_{\bar{p} = \mathrm{const}}} = \left[\frac{\partial \ln \bar{m}}{\partial \ln \bar{p}}\right]_{\bar{T}_s = \mathrm{const}} = \nu - \mu\frac{k}{r} \tag{6}$$

yielding different expressions for different pyrolysis laws and burning regimes.

For the reader's convenience, the following well-established results, when chemical reactions are concentrated at the burning surface and no phase transition occurs, are recalled:

1) The (intrinsic) stability condition in the ZN formulation[16,18,19] can be written as

$$\begin{cases} k < 1 & \text{always stable} \\ k > 1 & \text{stable if} \quad r > \dfrac{(k-1)^2}{k+1} \end{cases}$$

Table 2 Data matrix of baseline and modifications

p, atm	T_s, K	$Q_{\rm tra}$, cal/g	$T_{\rm tra}$, K	σ_p, K^{-1}	$\Delta \equiv \bar{T}_s - T_0 - (Q_{\rm tra}/c_c)$, K	$\alpha \equiv -(Q_{\rm tra}/c_c)/\Delta$	$\beta \equiv (T_{\rm tra} - T_0)/\Delta$	$\gamma \equiv -[c_c(T_{\rm tra} - T_0)/Q_{\rm tra}]$	r	k	$A = k/r$	$B = 1/k$	$n_s = \delta/r$
1	783.23	−18.3	513	0.003	540.68	0.103	0.398	3.877	0.229	1.456	6.358	0.687	0.063
10	868.73	−18.3	513	0.003	626.18	0.089	0.343	3.877	0.281	1.712	6.093	0.584	0.109
68	947	−18.3	513	0.003	704.45	0.079	0.305	3.877	0.334	1.947	5.829	0.514	0.143
1	783.23	−18.3	513	0.002	540.68	0.103	0.398	3.877	0.152	0.971	6.388	1.030	0.063
10	868.73	−18.3	513	0.002	626.18	0.089	0.343	3.877	0.188	1.142	6.075	0.876	0.109
68	947	−18.3	513	0.002	704.45	0.079	0.305	3.877	0.223	1.298	5.821	0.770	0.143
1	783.23	−18.3	513	0.004	540.68	0.103	0.398	3.877	0.305	1.941	6.364	0.515	0.063
10	868.73	−18.3	513	0.004	626.18	0.089	0.343	3.877	0.375	2.283	6.088	0.438	0.109
68	947	−18.3	513	0.004	704.45	0.079	0.305	3.877	0.446	2.596	5.821	0.385	0.143
1	783.23	−18.3	400	0.003	540.68	0.103	0.189	1.839	0.229	1.456	6.358	0.687	0.063
10	868.73	−18.3	400	0.003	626.18	0.089	0.163	1.839	0.281	1.712	6.093	0.584	0.109
68	947	−18.3	400	0.003	704.45	0.079	0.145	1.839	0.334	1.947	5.829	0.514	0.143
1	783.23	−18.3	600	0.003	540.68	0.103	0.559	5.446	0.229	1.456	6.358	0.687	0.063
10	868.73	−18.3	600	0.003	626.18	0.089	0.482	5.446	0.281	1.712	6.093	0.584	0.109
68	947	−18.3	600	0.003	704.45	0.079	0.429	5.446	0.334	1.947	5.829	0.514	0.143
1	783.23	−80	513	0.003	727.65	0.333	0.296	0.887	0.229	1.456	6.358	0.687	0.063
10	868.73	−80	513	0.003	813.15	0.298	0.264	0.887	0.281	1.712	6.093	0.584	0.109
68	947	−80	513	0.003	891.42	0.272	0.241	0.887	0.334	1.947	5.829	0.514	0.143
1	783.23	+40	513	0.003	364.02	−0.333	0.591	−1.774	0.152	0.971	6.388	1.030	0.063
10	868.73	+40	513	0.003	449.52	−0.270	0.478	−1.774	0.188	1.142	6.075	0.876	0.109
68	947	+40	513	0.003	527.79	−0.230	0.407	−1.774	0.223	1.298	5.821	0.770	0.143

and the equivalent FM formulation[33] of the parabolic boundary is

$$a = \frac{b(b-1)}{2} \tag{7}$$

being[31]

$$a = k/r \tag{8}$$

$$b = 1 + k/r - 1/r \tag{9}$$

2) The natural oscillatory frequency just at the stability boundary in the ZN formulation[16,18,19] can be written as

$$\Omega_{\rm bif} = \frac{\sqrt{k}}{r} = \sqrt{k}\frac{(k+1)}{(k-1)^2} \tag{10}$$

and the equivalent FM formulation[33] is

$$\Omega_{\rm bif} = [(b-1)/2]\sqrt{b(b-2)} \tag{11}$$

requiring $b > 2$ for real Ω.

3) The adiabatic pressure-driven frequency response function in the ZN formulation[17–19] can be written as

$$R_p(\Omega) = \frac{\nu + \delta(z_1 - 1)}{r(z_1 - 1) + k[(1/z_1) - 1] + 1} \tag{12}$$

and the equivalent Arrhenius FM formulation[23] is

$$R_p(\Omega) = \frac{n + (n_s/AB)(z_1 - 1)}{(1/AB)(z_1 - 1) + (1/B)[(1/z_1) - 1] + 1} \tag{13}$$

where[34]

$$A \equiv k/r, \qquad B \equiv 1/k, \qquad n \equiv \nu, \qquad n_s \equiv \delta/r \tag{14}$$

In both versions, the static limit R_p $(\Omega \to 0) = n$ (FM) or ν (ZN) is defined by the experimental steady-burning-rate law.

4) The ZN parameters can be converted into FM parameters by putting

$$k = \sigma_p(\bar{T}_s - T_0) = \frac{1}{B} = \frac{a}{1 + a - b} \tag{15}$$

$$r = \sigma_{T_s}\bar{T}_s = \frac{1}{AB} = \frac{1}{1 + a - b} \tag{16}$$

$$\nu = n \tag{17}$$

$$\mu = n_{T_s}\frac{\bar{T}_s}{\bar{T}_s - T_0} \tag{18}$$

Thus[32]

$$\frac{k}{r} = \frac{\sigma_p}{\sigma_{T_s}}\frac{\bar{T}_s - T_0}{\bar{T}_s} = A = a \tag{19}$$

and the ballistic Jacobian can be written as

$$\delta/r = n - n_{T_s} \cdot \sigma_p/\sigma_{T_s} \tag{20}$$

If one assumes a general form of the Arrhenius pyrolysis law (e.g., see Refs. 22–24, 35–38)

$$r_b = \tilde{A}_s p^{n_s} \exp(-\tilde{E}_s/\Re T_s) \tag{21}$$

then one can model the surface temperature sensitivity parameter r as

$$r = \sigma_p\left(\Re\bar{T}_s^2 \big/ \tilde{E}_s\right) \tag{22}$$

and $\delta/r = n_s$ (for discrete pyrolysis functions, see Ref. 32; see also the Appendix, of Ref. 39). Note that if one assumes a simple ($n_s = 0$) Arrhenius pyrolysis law

$$r_b = \tilde{A}_s \exp(-\tilde{E}_s/\Re T_s) \tag{23}$$

then the sensitivity parameter r is not modified [see Eq. (22)] but necessarily $\delta/r = n_s = 0$.

Under all circumstances, the accurate knowledge of σ_p is important but still a challenge; data collections can be found in Refs. 40–42.

III. Formulation of the Phase Transition Problem

The physical problem is sketched in Fig. 1. A one-dimensional strand of homogeneous material is assumed to be burning with a quasi-steady gas phase subjected to pressure changes in time only. Thermophysical properties are assumed to be, at most, pressure dependent. The strand is burning in a vessel at uniform pressure and is subjected to no radiation, no velocity coupling, and no external forces. Assume no condensed-phase chemical activity, except the chemical reactions concentrated at the burning surface and at the phase transition plane located somewhere in depth. Define a

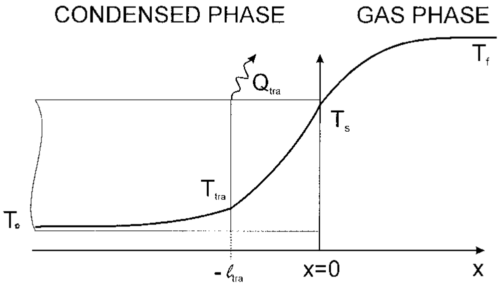

Fig. 1 Schematic of the physical problem.

Cartesian axis with its origin anchored at the burning surface and positive in the gas-phase direction. The phase transition, be it solid to solid or solid to liquid, is assumed to be concentrated at the position $x = -\ell_{\text{tra}}(t)$, where the transition temperature T_{tra} is observed. In general, the phase transition will take place with a (net) heat release Q_{tra} (positive if exothermic). Both parameters T_{tra} and Q_{tra} are considered to be known and fixed quantities. For the sake of simplicity, thermophysical properties are assumed to be unaffected by the phase transition.

Let the condensed phase ($x < 0$) be a semi-infinite slab of uniform and isotropic composition, and T_0 its initial temperature. Only the particular case of pressure-driven burning is considered. Under these circumstances, the energy conservation equation is simply

$$\frac{\partial T}{\partial t} + r_b \frac{\partial T}{\partial x} = \alpha_c \frac{\partial^2 T}{\partial x^2} \tag{24}$$

The boundary conditions can be written over the thickness $-\infty < x < -\ell_{\text{tra}}$ as

$$T(x \to -\infty, t) = T_0 \tag{25}$$

$$T(x \to -\ell_{\text{tra}}, t) = T_{\text{tra}} \tag{26}$$

and over the thickness $-\ell_{\text{tra}} < x < 0$ as

$$T(x \to -\ell_{\text{tra}}, t) = T_{\text{tra}} \tag{27}$$

$$T(x = 0, t) = T_s \tag{28}$$

At the position $x = -\ell_{\text{tra}}(t)$, energy conservation requires matching of the two thermal profiles

$$k_c \left| \frac{\partial T}{\partial x} \right|_{-\ell_{\text{tra}}^-} = k_c \left| \frac{\partial T}{\partial x} \right|_{-\ell_{\text{tra}}^+} + \rho_c \left(r_b + \frac{d\ell_{\text{tra}}}{dt} \right) Q_{\text{tra}} \tag{29}$$

If pressure and initial temperature are taken as independent variables, then, under steady state,

$$\bar{r}_b = \bar{r}_b(\bar{p}, T_0) \tag{30}$$

$$\bar{T}_s = \bar{T}_s(\bar{p}, T_0) \tag{31}$$

Likewise, under steady state, the thermal gradient at the condensed-phase side of the burning surface is

$$\bar{f} \equiv \left[\frac{d\bar{T}}{dx} \right]_{x=0^-} = \frac{\bar{r}_b}{\alpha_c} \left(\bar{T}_s - T_0 - \frac{Q_{\text{tra}}}{c_c} \right) \tag{32}$$

taking explicitly into account the heat release associated with phase transition. Under both steady and nonsteady operations, introducing pressure and thermal gradient as independent variables, one can write

$$r_b = r_b(p, f) \tag{33}$$

$$T_s = T_s(p, f) \tag{34}$$

A. Steady-State Solution

For the steady-state part of the problem, one finds for the thermal profile

1) $-\infty < x < -\bar{\ell}_{\text{tra}}$

$$\bar{T}(x) = T_0 + (T_{\text{tra}} - T_0) \exp[\bar{r}_b/\alpha_c(x + \bar{\ell}_{\text{tra}})] \tag{35}$$

2) $-\bar{\ell}_{\text{tra}} < x < 0$

$$\bar{T}(x) = \frac{T_{\text{tra}} - \bar{T}_s \exp(-\bar{r}_b/\alpha_c\bar{\ell}_{\text{tra}}) + (\bar{T}_s - T_{\text{tra}}) \exp(\bar{r}_b/\alpha_c x)}{1 - \exp(-\bar{r}_b/\alpha_c\bar{\ell}_{\text{tra}})} \tag{36}$$

Matching at the transition location yields

3) $x = -\bar{\ell}_{\text{tra}}$

$$k_c \left[\frac{d\bar{T}}{dx} \right]_{-\bar{\ell}_{\text{tra}}^-} = k_c \left[\frac{d\bar{T}}{dx} \right]_{-\bar{\ell}_{\text{tra}}^+} + \rho_c \bar{r}_b Q_{\text{tra}} \tag{37}$$

which, by replacing the proper thermal gradients, in turn gives

$$\frac{\bar{r}_b}{\alpha_c}(T_{\text{tra}} - T_0) = \frac{\bar{r}_b}{\alpha_c} \frac{\bar{T}_s - T_{\text{tra}}}{1 - \exp(-\bar{r}_b/\alpha_c\bar{\ell}_{\text{tra}})} \exp(-\bar{r}_b/\alpha_c\bar{\ell}_{\text{tra}}) + \frac{\bar{r}_b}{\alpha_c} \frac{Q_{\text{tra}}}{c_c} \tag{38}$$

Thus, the transition location inside the condensed phase is defined by

$$\bar{\ell}_{\text{tra}} = \frac{\alpha_c}{\bar{r}_b} \ln \frac{\bar{T}_s - T_0 - Q_{\text{tra}}/c_c}{T_{\text{tra}} - T_0 - Q_{\text{tra}}/c_c} = \frac{\alpha_c}{\bar{r}_b} \ln \left(\frac{1}{\alpha + \beta} \right) \tag{39}$$

where (cf. the corresponding definitions in Ref. 29)

$$\alpha \equiv -\frac{Q_{\text{tra}}/c_c}{\bar{T}_s - T_0 - Q_{\text{tra}}/c_c} = -\frac{Q_{\text{tra}}/c_c}{\Delta} \tag{40}$$

$$\beta \equiv \frac{T_{\text{tra}} - T_0}{\bar{T}_s - T_0 - Q_{\text{tra}}/c_c} = \frac{T_{\text{tra}} - T_0}{\Delta} \tag{41}$$

$$\gamma \equiv \frac{\beta}{\alpha} = -\frac{c_c(T_{\text{tra}} - T_0)}{Q_{\text{tra}}} \tag{42}$$

$$\Delta \equiv \bar{T}_s - T_0 - \frac{Q_{\text{tra}}}{c_c} \tag{43}$$

For the selected test case (see Table 1), the pressure dependence of the relevant thermophysical parameters is illustrated in Fig. 2. Parameter $\Delta \equiv \bar{T}_s - T_0 - Q_{\text{tra}}/c_c$ shows a fair increase with pressure due to increasing surface temperature; both parameters $\alpha \equiv -(Q_{\text{tra}}/c_c)/\Delta$ and $\beta \equiv (T_{\text{tra}} - T_0)/\Delta$ show a slight decrease for increasing pressure, again due to increasing surface temperature. For the assumptions made, pressure effects cannot exist for $\gamma \equiv \beta/\alpha = -c_c(T_{\text{tra}} - T_0)/Q_{\text{tra}}$. Typical trends of the nondimensional transition depth $\bar{\ell}_{\text{tra}}\bar{r}_b/\alpha_c$ are illustrated in Fig. 3: $\bar{\ell}_{\text{tra}}\bar{r}_b/\alpha_c$

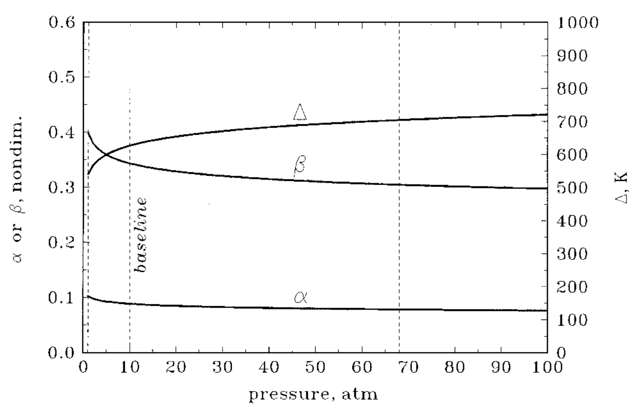

Fig. 2 Dependence of thermophysical parameters α, β, and Δ on pressure in the test case for the indicated set of operating parameters.

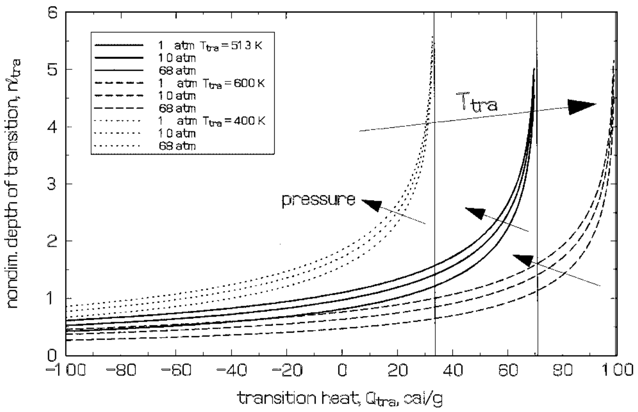

Fig. 3 Dependence of nondimensional transition depth on operating conditions in the test case for the indicated set of operating parameters.

is seen to increase with increasing Q_{tra}, increasing pressure, and decreasing T_{tra}. Notice that a limiting value of $Q_{\text{tra}} \leq c_c(T_{\text{tra}} - T_0)$ exists for which the denominator of the logarithmic factor in Eq. (39) vanishes. This bound concerns only exothermic processes and is more severe for smaller T_{tra}, as manifest in Fig. 3.

B. Unsteady Solution

To solve the nonsteady part of the problem, first the linear approximation of the problem is considered[19]:

$$r_b(t) = \bar{r}_b + r_b' \exp(i\omega t) \qquad r_b' \ll \bar{r}_b \tag{44}$$

$$T_s(t) = \bar{T}_s + T_s' \exp(i\omega t) \qquad T_s' \ll \bar{T}_s \tag{45}$$

$$p(t) = \bar{p} + p' \exp(i\omega t) \qquad p' \ll \bar{p} \tag{46}$$

$$f(t) = \bar{f} + f' \exp(i\omega t) \qquad f' \ll \bar{f} \tag{47}$$

$$\ell_{\text{tra}}(t) = \bar{\ell}_{\text{tra}} + \ell_{\text{tra}}' \exp(i\omega t) \qquad \ell_{\text{tra}}' \ll \bar{\ell}_{\text{tra}} \tag{48}$$

$$T(x,t) = \bar{T}(x) + T'(x) \exp(i\omega t) \qquad T'(x) \ll \bar{T}(x) \tag{49}$$

Then, one finds for the thermal profile:

1) $-\infty < x < -\ell_{\text{tra}}$

$$\frac{\partial}{\partial t}[T'(x)\exp(i\omega t)] + [\bar{r}_b + r_b'\exp(i\omega t)]\frac{\partial}{\partial x}[\bar{T}(x) + T'(x)\exp(i\omega t)] \tag{50}$$

$$= \alpha_c \frac{\partial^2}{\partial x^2}[\bar{T}(x) + T'(x)\exp(i\omega t)] \tag{51}$$

By variable separation, one gets the steady portion whose solution is again Eq. (35) and the unsteady portion

$$i\omega T'(x) + \bar{r}_b \frac{\partial}{\partial x}T'(x) - \alpha_c \frac{\partial^2}{\partial x^2}T'(x) = -r_b' \frac{\partial}{\partial x}\bar{T}(x) \tag{52}$$

whose general solution is

$$T'(-\infty < x < -\ell_{\text{tra}}) = C_3 \exp\left(\frac{\bar{r}_b}{\alpha_c} z_1 x\right) + C_4 \exp\left(\frac{\bar{r}_b}{\alpha_c} z_2 x\right) - \frac{\bar{r}_b}{\alpha_c}\frac{r_b'}{i\omega}\frac{T_{\text{tra}} - T_0}{\alpha + \beta}\exp\left(\frac{\bar{r}_b}{\alpha_c}x\right) \tag{53}$$

2) $-\ell_{\text{tra}} < x < 0$

$$\frac{\partial}{\partial t}[T'(x)\exp(i\omega t)] + [\bar{r}_b + r_b'\exp(i\omega t)]\frac{\partial}{\partial x}[\bar{T}(x) + T'(x)\exp(i\omega t)] = \alpha_c \frac{\partial^2}{\partial x^2}[\bar{T}(x) + T'(x)\exp(i\omega t)] \tag{54}$$

By variable separation, one gets the steady portion whose solution is again Eq. (36) and the unsteady portion

$$i\omega T'(x) + \bar{r}_b \frac{\partial}{\partial x}T'(x) - \alpha_c \frac{\partial^2}{\partial x^2}T'(x) = -r_b' \frac{\partial}{\partial x}\bar{T}(x) \tag{55}$$

whose general solution is

$$T'(-\ell_{\text{tra}} < x < 0) = C_1 \exp[(\bar{r}_b/\alpha_c)z_1 x] + C_2 \exp[(\bar{r}_b/\alpha_c)z_2 x] - (\bar{r}_b/\alpha_c)(r_b'/i\omega)\Delta \exp[(\bar{r}_b/\alpha_c)x] \tag{56}$$

where

$$z_{1,2} \equiv \frac{1 \pm \sqrt{1 + 4i\omega\alpha_c/\bar{r}_b^2}}{2} \tag{57}$$

The constants C_1, C_2, C_3, and C_4 are to be evaluated by satisfying the following constraints:

$$T'(x \to -\infty) = 0 \tag{58}$$

$$-\left[\frac{\partial \bar{T}(x)}{\partial x}\right]_{x=-\bar{\ell}_{\text{tra}}^-} \ell_{\text{tra}}' + T'\left(x = -\bar{\ell}_{\text{tra}}^-\right) = 0 \tag{59}$$

$$-\left[\frac{\partial \bar{T}(x)}{\partial x}\right]_{x=-\bar{\ell}_{\text{tra}}^+} \ell_{\text{tra}}' + T'\left(x = -\bar{\ell}_{\text{tra}}^+\right) = 0 \tag{60}$$

$$T'(x = 0) = T_s' \tag{61}$$

In addition, energy conservation is required both at the position $x = -\ell_{\text{tra}}(t)$, yielding matching of the fluctuating portions of the thermal profile

$$\left[-\frac{\partial^2 \bar{T}}{\partial x^2}\ell_{\text{tra}}' + \frac{\partial T'}{\partial x}\right]_{x=-\bar{\ell}_{\text{tra}}^-} = \left[-\frac{\partial^2 \bar{T}}{\partial x^2}\ell_{\text{tra}}' + \frac{\partial T'}{\partial x}\right]_{x=-\bar{\ell}_{\text{tra}}^+} - \frac{Q_{\text{tra}}}{c_c}\frac{r_b' + i\omega\ell_{\text{tra}}'}{\bar{r}_b}\frac{\bar{r}_b}{\alpha_c}$$

and at the burning surface yielding the fluctuating portion of the thermal gradient

$$\left[\frac{\partial T'}{\partial x}\right]_{x=0^-} = f'$$

By replacing the appropriate thermal profiles, one obtains

$$T'(x \to -\infty) = 0 \tag{62}$$

$$C_3 \exp[-(\bar{r}_b/\alpha_c)z_1\bar{\ell}_{\text{tra}}] - (\bar{r}_b/\alpha_c)(r_b'/i\omega)(T_{\text{tra}} - T_0) = (\bar{r}_b/\alpha_c)(T_{\text{tra}} - T_0)\ell_{\text{tra}}' \tag{63}$$

$$C_1 \exp[-(\bar{r}_b/\alpha_c)z_1\bar{\ell}_{\text{tra}}] + C_2 \exp[-(\bar{r}_b/\alpha_c)z_2\bar{\ell}_{\text{tra}}] - (\bar{r}_b/\alpha_c)(r_b'/i\omega)\Delta\exp[-(\bar{r}_b/\alpha_c)\bar{\ell}_{\text{tra}}] = (\bar{r}_b/\alpha_c)[T_{\text{tra}} - T_0 - (Q_{\text{tra}}/c_c)]\ell_{\text{tra}}' \tag{64}$$

$$T'(x = 0) = C_1 + C_2 - (\bar{r}_b/\alpha_c)(r_b'/i\omega)\Delta = T_s' \tag{65}$$

$$z_1 C_1 \exp\left(-\frac{\bar{r}_b}{\alpha_c}z_1\bar{\ell}_{\text{tra}}\right) + z_2 C_2 \exp\left(-\frac{\bar{r}_b}{\alpha_c}z_2\bar{\ell}_{\text{tra}}\right) - z_1 C_3 \exp\left(-\frac{\bar{r}_b}{\alpha_c}z_1\bar{\ell}_{\text{tra}}\right) - \frac{\bar{r}_b}{\alpha_c}\frac{r_b'}{i\omega}\Delta\exp\left(-\frac{\bar{r}_b}{\alpha_c}\bar{\ell}_{\text{tra}}\right) + \frac{\bar{r}_b}{\alpha_c}\frac{r_b'}{i\omega}(T_{\text{tra}} - T_0) = \frac{\bar{r}_b}{\alpha_c}\frac{Q_{\text{tra}}}{c_c}\ell_{\text{tra}}' - \frac{\bar{r}_b}{\alpha_c}\frac{Q_{\text{tra}}}{c_c}\frac{r_b' + i\omega\ell_{\text{tra}}'}{\bar{r}_b} \tag{66}$$

$$\left[\frac{\partial T'(x)}{\partial x}\right]_{0^-} = \frac{\bar{r}_b}{\alpha_c} z_1 C_1 + \frac{\bar{r}_b}{\alpha_c} z_2 C_2 - \left(\frac{\bar{r}_b}{\alpha_c}\right)^2 \frac{r_b'}{i\omega}\Delta = f' \quad (67)$$

By enforcing the boundary condition of Eq. (62), one finds that $C_4 = 0$, whereas Eq. (64) gives $\ell'_{\text{tra}} = \ell'_{\text{tra}}(C_1, C_2)$ and Eq. (63) gives $C_3 = C_3(\ell'_{\text{tra}}) = C_3(C_1, C_2)$. By replacing ℓ'_{tra} and C_3 in Eq. (66) and taking into account Eq. (65), one can evaluate C_1, C_2. At this point, Eq. (67) is fully determined, which connects the three fluctuating values of burning rate, surface temperature, and thermal gradient. This equation is used to define the intrinsic stability boundary, as discussed next.

C. Intrinsic Stability

The condition of solvability of the homogeneous system comprising the 1) energy boundary condition at the condensed-phase side of the burning surface, 2) fluctuating burning-rate dependence on the fluctuating thermal gradient, and 3) fluctuating surface temperature on the fluctuating thermal gradient (see Ref. 18, p. 82) is

$$\begin{vmatrix} A_1 & A_2 & A_3 \\ 1 & 0 & -\dfrac{k/(1-\alpha)}{k/(1-\alpha)+r-1} \\ 0 & 1 & -\dfrac{r}{k/(1-\alpha)+r-1} \end{vmatrix} = 0$$

where

$$A_1 = \frac{(\alpha+\beta)^{1-z_1}}{z_1} + \frac{(z_1-1)(\alpha+\beta)^{z_1}}{(z_1+2\gamma)z_1-\gamma} \quad (68)$$

$$A_2 = z_1(\alpha+\beta)^{1-z_1} + \frac{(\alpha+\beta)^{z_1}(z_1-1)^3}{(z_1+2\gamma)z_1-\gamma} \quad (69)$$

$$A_3 = -(\alpha+\beta)^{1-z_1} + \frac{(\alpha+\beta)^{z_1}(z_1-1)^2}{(z_1+2\gamma)z_1-\gamma} \quad (70)$$

This condition leads to a complex equation describing the linear stability boundary and associated oscillatory burning frequency, at constant pressure, of the stated problem

$$rZ_r + k[Z_k/(1-\alpha)] + Z = 0 \quad (71)$$

Here r and k are real while Z_r, Z_k, Z are coefficients depending on the nondimensional frequency Ω and thermophysical properties of the energetic material (α, β, γ)

$$Z_r = z_1 - 1 + z_1\frac{(z_1-1)^2(\alpha+\beta)^{2z_1-1}}{z_1^2+\gamma(2z_1-1)} \quad (72)$$

$$Z_k = \frac{1}{z_1} - 1 + z_1\frac{(z_1-1)(\alpha+\beta)^{2z_1-1}}{z_1^2+\gamma(2z_1-1)} \quad (73)$$

$$Z = 1 - \frac{(z_1-1)^2(\alpha+\beta)^{2z_1-1}}{z_1^2+\gamma(2z_1-1)} \quad (74)$$

Notice that the former (with no transition) μ and k parameters now are defined more generally as

$$\mu' \equiv \frac{1}{(\bar{T}_s - T_0 - Q_{\text{tra}}/c_c)}\left[\frac{\partial \bar{T}_s}{\partial \ln \bar{p}}\right]_{T_0=\text{const}} \quad (75)$$

$$k' \equiv (\bar{T}_s - T_0 - Q_{\text{tra}}/c_c)\left[\frac{\partial \ln \bar{m}}{\partial T_0}\right]_{\bar{p}=\text{const}} \quad (76)$$

but the pressure Jacobian [see Eq. (5)] is not affected; for $Q_{\text{tra}} \to 0$, i.e., phase transition with no heat release, the former definitions are recovered. Notice also that for $Q_{\text{tra}} \to 0$, i.e., $\alpha \to 0$, one finds

$$Z_r \to z_1 - 1 \quad (77)$$

$$Z_k \to (1/z_1) - 1 \quad (78)$$

$$Z \to 1 \quad (79)$$

thus recovering the previous result (see Ref. 19, p. 619)

$$r(z_1-1) + k[(1/z_1)-1] + 1 = 0 \quad (80)$$

In turn, this leads to the explicit solution (cf. Sec. II)

$$r = \frac{(k-1)^2}{k+1} \quad \text{with} \quad k > 1 \quad (81)$$

$$\Omega_{\text{bif}} = \sqrt{k}\frac{(k+1)}{(k-1)^2} \quad (82)$$

Unfortunately, in this instance, an explicit solution of Eq. (71) is no longer possible, but a parametric representation in the nondimensional frequency Ω can be implemented. Multiplying Eq. (71) separately by Z_k^* and Z_r^*, the following complex relationships are obtained:

$$rZ_rZ_k^* + [k/(1-\alpha)]Z_kZ_k^* + ZZ_k^* = 0$$

$$rZ_rZ_r^* + [k/(1-\alpha)]Z_kZ_r^* + ZZ_r^* = 0 \quad (83)$$

Imaginary parts of Eqs. (83) give

$$r = \frac{\text{Im}(-Z\cdot Z_k^*)}{\text{Im}(Z_r\cdot Z_k^*)}, \qquad k = (1-\alpha)\frac{\text{Im}(-Z\cdot Z_r^*)}{\text{Im}(Z_k\cdot Z_r^*)} \quad (84)$$

Thus, Eqs. (84) are parametric representations of the stability boundary in the parameter Ω. The values k and r given by Eqs. (84), for Ω spanning from 0 to infinity, describe a line that is just the wanted stability boundary in the k, r plane. Notice that parameter k without transition is replaced by $k/(1-\alpha)$ when transition occurs.

Representative applications are discussed in Sec. IV.A.

D. Linear Frequency Response Function

The linear frequency response function is defined as

$$R_p(\Omega) \equiv (m'/\bar{m})/(p'/\bar{p}) \quad (85)$$

and, for adiabatic burning, is found to be

$$R_p(\Omega) = \frac{\nu Z + \delta Z_r}{rZ_r + k[Z_k/(1-\alpha)] + Z} \quad (86)$$

Notice that, for $\alpha \to 0$, i.e., phase transition with no heat release,

$$Z_r \to z_1 - 1 \quad (87)$$

$$Z_k \to (1/z_1) - 1 \quad (88)$$

$$Z \to 1 \quad (89)$$

thus recovering the previous ZN result (cf. Sec. II)

$$R_p(\Omega) = \frac{\nu + \delta(z_1-1)}{r(z_1-1) + k[(1/z_1)-1] + 1} \quad (90)$$

Notice that the denominator of Eq. (86) coincides with Eq. (71); as already noticed by Culick,[23] this boundary corresponds to the condition of unbounded response of the burning propellant even for vanishing fluctuations of the forcing term; i.e., it is the intrinsic stability boundary.

Representative applications are discussed in Sec. IV.B.

IV. Representative Results

For the sake of completeness, the pressure dependence of the sensitivity parameters k and r is illustrated in Fig. 4: In both cases, the increase with pressure is due to increasing surface temperature while σ_p is kept constant. A more realistic σ_p, decreasing with pressure (see Fig. 5), contrasts this trend by opposing the increase of surface temperature and thus favoring stability (see discussion in Sec. IV.A). Unfortunately, an exact definition of the σ_p value requires an accuracy of ballistic property measurements that cannot be obtained at this time.

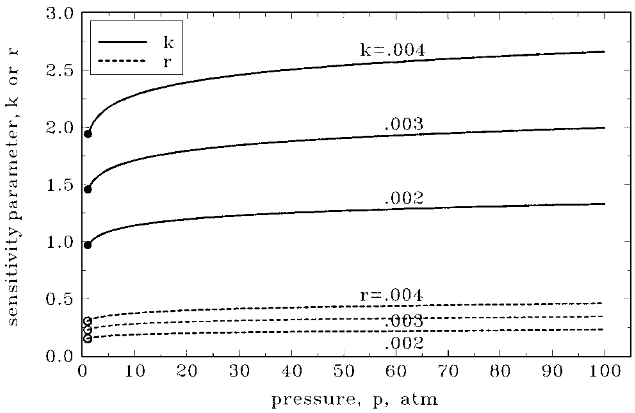

Fig. 4 Dependence of ZN parameters *k* and *r* on operating pressure for constant σ_p.

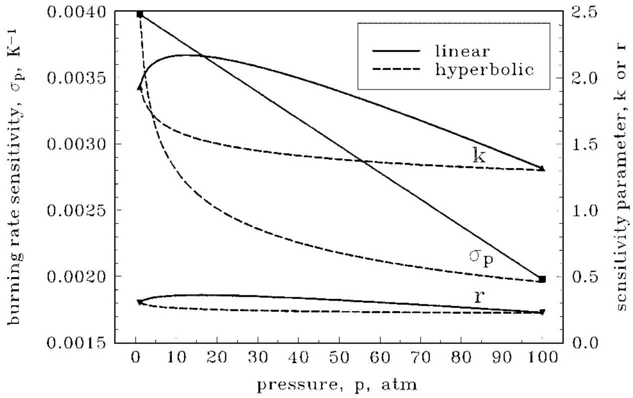

Fig. 5 Dependence of ZN parameters *k* and *r* on operating pressure for σ_p decreasing in pressure.

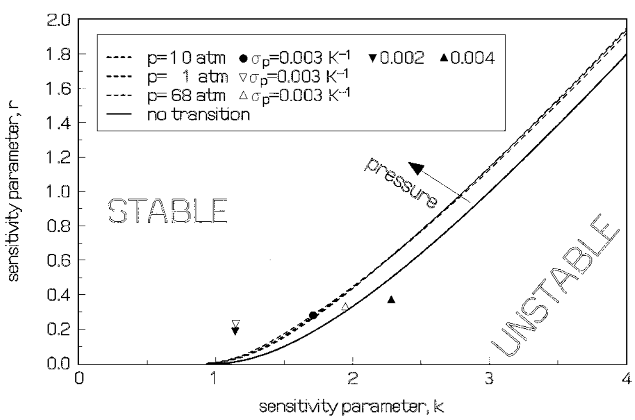

Fig. 6 QSHOD intrinsic stability map for pressure-driven burning, showing the selected test case and several modifications.

A. Intrinsic Stability

The intrinsic linear stability boundary is affected by the phase transition inclusion, as shown in Figs. 6–10. For the enforced set of operating conditions (a typical endothermic transition), the stability region for a given set of k, r parameters apparently is decreased with respect to the no-transition boundary, with little sensitivity to pressure and more sensitivity to $\gamma \equiv \beta/\alpha = -c_c(T_{\text{tra}} - T_0)/Q_{\text{tra}}$. However, this observation might be misleading if one neglects to reexamine simultaneously the possible change of the corresponding operating point on the stability plot.

Several cases are illustrated in Fig. 6. For the selected test case (see Table 1), the corresponding operating point ($\sigma_p = 0.003$ K^{-1} at 10 atm) accidentally falls very close to the new stability boundary (cf. frequency response functions as portrayed in Figs. 11–18).

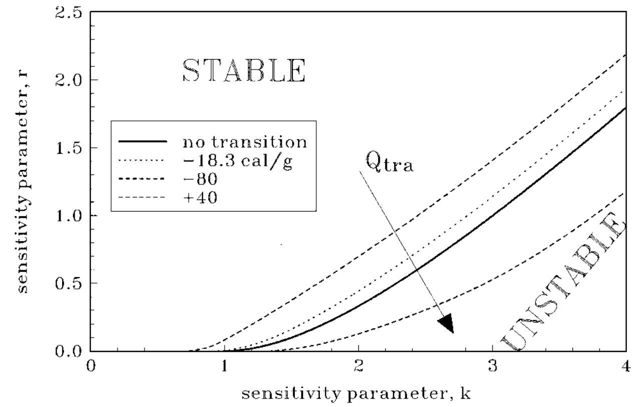

Fig. 7 QSHOD intrinsic stability map for pressure-driven burning, showing dependence of stability boundary on the transition heat release (Q_{tra} parametrically varying from − 80 to − 18.3 to +40 cal/g) for the indicated set of operating parameters.

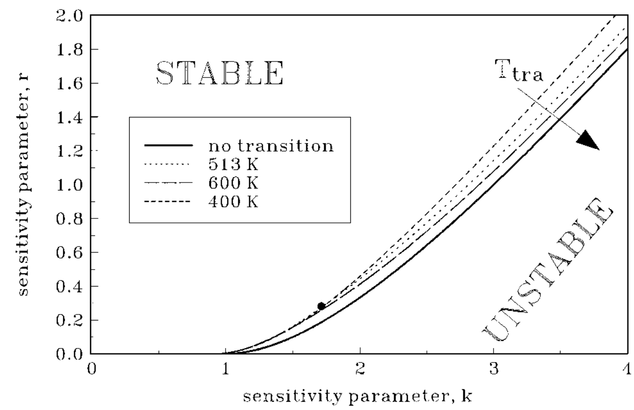

Fig. 8 QSHOD intrinsic stability map for pressure-driven burning, showing dependence of stability boundary on the transition temperature (T_{tra} parametrically varying from 400 to 600 K) for the indicated set of operating parameters.

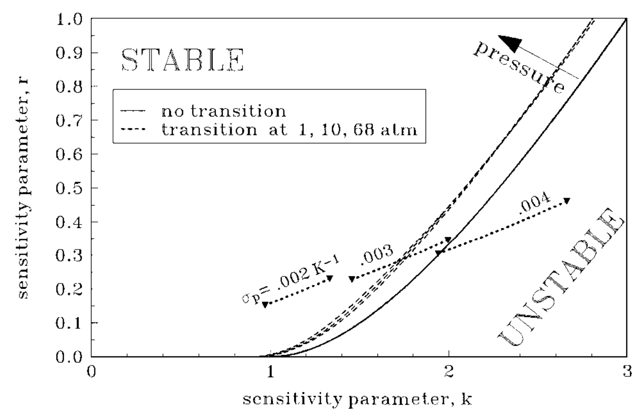

Fig. 9 QSHOD intrinsic stability map for pressure-driven burning, showing loss of stability of the operating point, ranging from 1 to 100 atm, when pressure and/or σ_p are parametrically increased for the indicated set of operating parameters.

Changing either pressure or σ_p (see Table 2) strongly affects the stability features. An increase of pressure (from 10 to 68 atm) at constant σ_p or an increase of σ_p (from 0.003 to 0.004 K^{-1}) at constant pressure is destabilizing; vice versa, a decrease of pressure (from 10 to 1 atm) at constant σ_p or a decrease of σ_p (from 0.003 to 0.002 K^{-1}) at constant pressure is stabilizing. By parametrically varying the phase transition heat release (see Fig. 7), the stability region apparently is decreased for endothermic (likely) transition but increased for exothermic (unlikely) transition with respect to the no-transition boundary; these effects are more evident for larger

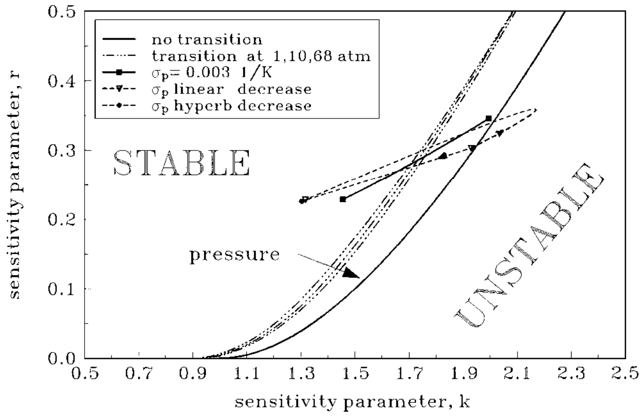

Fig. 10 QSHOD intrinsic stability map for pressure-driven burning, showing gain of stability of the operating point for σ_p decreasing in pressure for the indicated set of operating parameters.

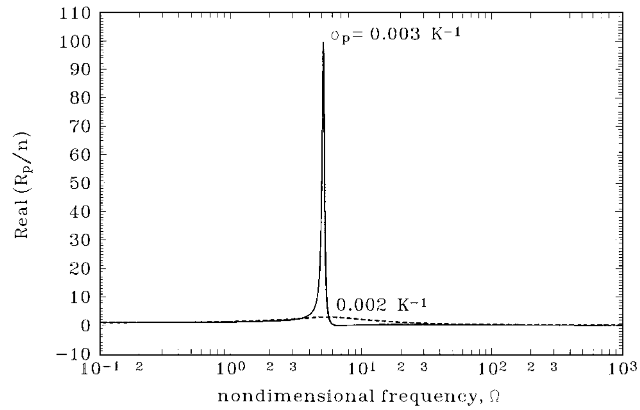

Fig. 13 Frequency response (real part) for pressure-driven burning showing the effect of a σ_p decrease from 0.003 to 0.002 K^{-1} for p = 10 atm, T_{tra} = 513 K, and Q_{tra} = − 18.3 cal/g.

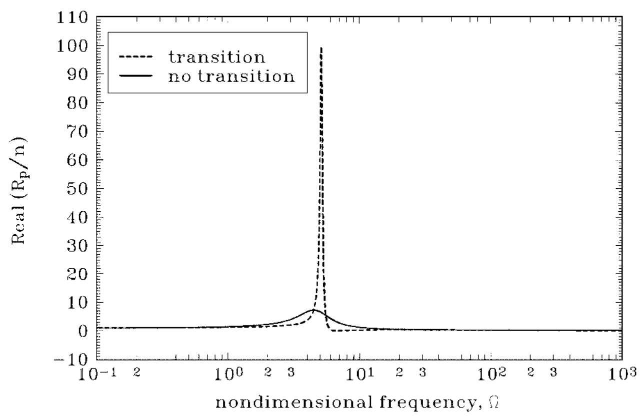

Fig. 11 Frequency response (real part) for pressure-driven burning, showing the effect of phase transition for the test case.

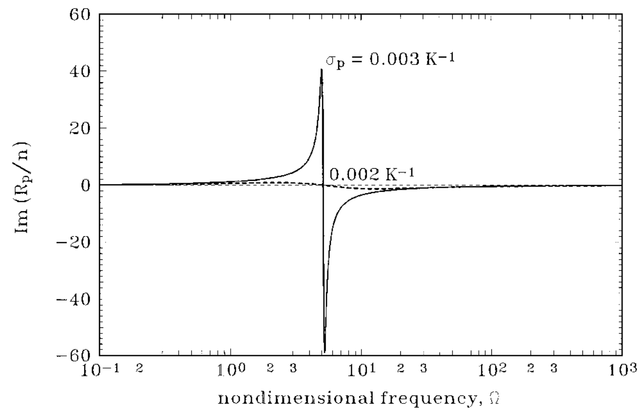

Fig. 14 Frequency response (imaginary part) for pressure-driven burning, showing the effect of a σ_p decrease from 0.003 to 0.002 K^{-1} for p = 10 atm, T_{tra} = 513 K, and Q_{tra} = − 18.3 cal/g.

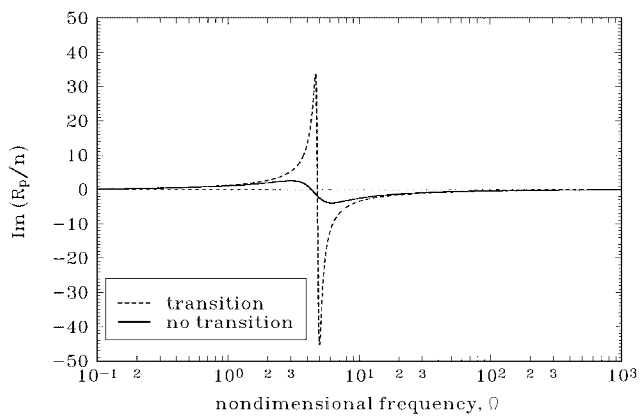

Fig. 12 Frequency response (imaginary part) for pressure-driven burning, showing the effect of phase transition for the test case.

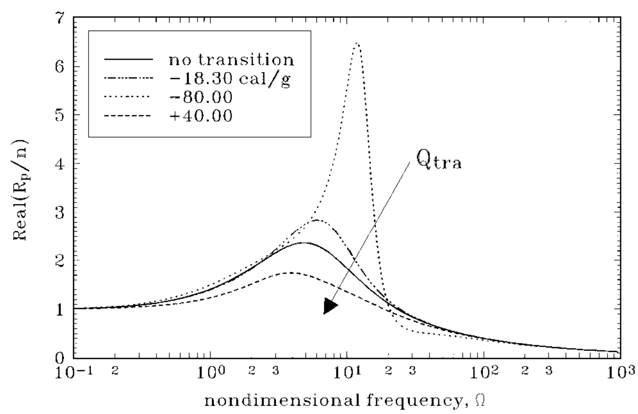

Fig. 15 Frequency response (real part) for pressure-driven burning, showing the effect of the transition heat release (Q_{tra} parametrically varying from − 80 to − 18.3 to +40 cal/g) for σ_p = 0.002 K^{-1}, p = 10 atm, and T_{tra} = 513 K.

values of Q_{tra}, but, anyway, exothermicity is upper bounded (see Sec. III.A). By parametrically varying the phase transition temperature (see Fig. 8), the main effect seems again to be an apparent shrinking of the stability region; the effect is stronger for decreasing T_{tra} but overall less pronounced than for Q_{tra}. The effect of σ_p assumed to be constant is shown parametrically in Fig. 9 as loss of stability for increasing σ_p, while the operating point ranges from 1 to 100 atm. A more complex behavior is shown in Fig. 10 for σ_p assumed to be decreasing in pressure according to the laws implemented in Fig. 5: For increasing pressure, a linearly decreasing σ_p yields instability and then stability; a faster σ_p decrease yields stability.

B. Linear Frequency Response Function

Typical trends for the test case and selected modifications (see Table 2) are illustrated in Figs. 11–18. A direct comparison between frequency response functions computed for the test case with or without phase transition, for the particular operating point selected in Fig. 8, is shown in Figs. 11 and 12 (respectively, real and imaginary parts). Taking into account phase transition brings about a much stronger peak response, although the peak frequency is affected only slightly; this is a consequence of the selected operating point falling almost on the stability boundary (cf. Fig. 6). As a matter of fact, for the selected test case, a decrease of σ_p (from 0.003 to 0.002

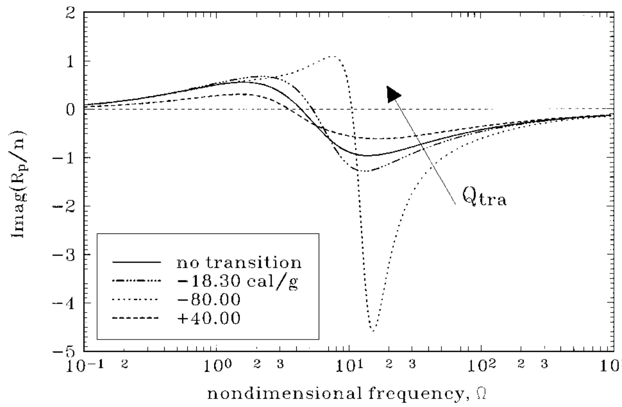

Fig. 16 Frequency response (imaginary part) for pressure-driven burning, showing the effect of the transition heat release (Q_{tra} parametrically varying from − 80 to − 18.3 to +40 cal/g) for σ_p = 0.002 K^{-1}, p = 10 atm, and T_{tra} = 513 K.

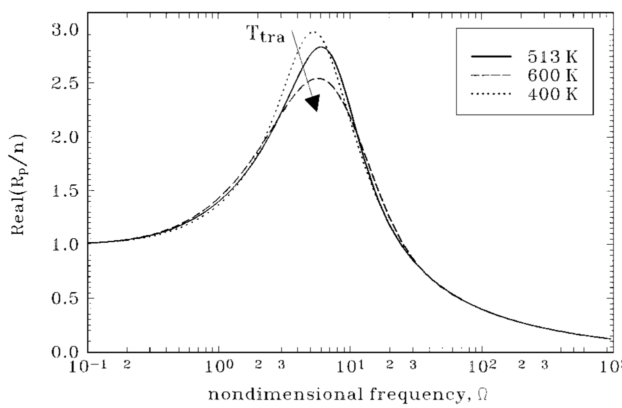

Fig. 17 Frequency response (real part) for pressure-driven burning, showing the effect of the transition temperature (T_{tra} parametrically varying from 400 to 600 K) for σ_p = 0.002 K^{-1}, p = 10 atm, and Q_{tra} = − 18.3 cal/g.

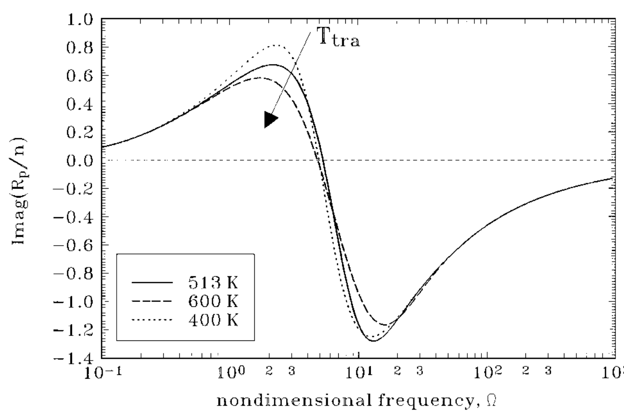

Fig. 18 Frequency response (imaginary part) for pressure-driven burning, showing the effect of the transition temperature (T_{tra} parametrically varying from 400 to 600 K) for σ_p = 0.002 K^{-1}, p = 10 atm, and Q_{tra} = − 18.3 cal/g.

K^{-1}) implies a strong reduction of the response, as clearly shown in Figs. 13 and 14. The effect of Q_{tra} is illustrated in Figs. 15 and 16 for $\sigma_p = 0.002$ K^{-1}: For this case, increasing or decreasing Q_{tra} yields a much weaker peak response. The effect of T_{tra} is illustrated in Figs. 17 and 18 for $\sigma_p = 0.002$ K^{-1}: For this case, increasing or decreasing T_{tra} yields a less pronounced peak response.

The fact that the heat release associated with the phase transition for the test case is a small fraction of the overall condensed-phase heat sink ($\alpha \ll 1$) should not be misunderstood. The unifying interpretation is that phase transition, as any other effect, affects the response function more when the operating point is closer to the intrinsic stability boundary. Parameters favoring the displacement of the operating point far away from the stability boundary (low σ_p, low pressures, etc.) will manifest few consequences on the frequency response function, and vice versa.

V. Conclusions

Frequency response functions and the intrinsic stability boundary were obtained for a concentrated phase transition in the condensed phase with constant thermophysical properties. Both endothermic and exothermic phase transitions are allowed. The results of the classical no-transition configuration are recovered as a limiting case. The destabilizing effects of large σ_p, or σ_p not decreasing with pressure, are manifest. Thus, the importance of accurate experimental determination of the sensitivity parameters, especially σ_p, is stressed.

An extension including the simultaneous change of thermophysical properties is in progress.

Acknowledgments

The financial support of ASI Contract ARS-96-130 for this investigation is acknowledged gratefully. The financial support of Cariplo Scientific Foundation–Landau Network Centro Volta, Como, Italy, for the research activities conducted by Boris V. Novozhilov as Visiting Professor at Politecnico di Milano, during the period March–June 1997 is acknowledged gratefully. Presented as a paper at the International Workshop on Combustion Instability of Solid Propellants and Rocket Motors, Politecnico di Milano, Milan, Italy, 16–18 June 1997.

References

[1]DeLuca, L. T., and Novozhilov, B. V., "On Some Contradictions between Theory and Experiments in Solid Propellant Burning," Politecnico di Milano, Paper 97-05-03, June 1997.

[2]Whittaker, A. G., and Barham, D. C., "Surface Temperature Measurements on Burning Solids," *Journal of Physical Chemistry*, Vol. 68, No. 1, 1964, pp. 196–199.

[3]Meyer. R., *Explosives*, 2nd ed., Verlag Chemie, Weinheim, Germany, 1981, pp. 16–18.

[4]Markowitz, M. M., and Boryta, D. A., "Some Aspects of the Crystallographic Transition of AP," *ARS Journal*, Vol. 32, No. 12, 1962, pp. 1941–1942.

[5]Guirao, C., and Wiliams, F. A., "A Model for Ammonium Perchlorate Deflagration Between 20 and 100 atm," *AIAA Journal*, Vol. 9, No. 7, 1971, pp. 1345–1356.

[6]Boggs, T. L., "The Thermal Behavior of Cyclotrimethylenetrinitramine (RDX) and Cyclotetramethylenetetranitramine (HDX)," *Fundamentals of Solid Propellant Combustion*, edited by K. K. Kuo and M. Summerfield, Progress in Astronautics and Aeronautics, AIAA, Washington, DC, 1984, pp. 121–175.

[7]Fifer, R. A., "Chemistry of Nitrate Ester and Nitramine Propellants," *Fundamentals of Solid Propellant Combustion*, edited by K. K. Kuo and M. Summerfield, Progress in Astronautics and Aeronautics, AIAA, Washington, DC, 1984, pp. 177–237.

[8]Liau, Y. C., and Yang, V., "Analysis of RDX Monopropellant Combustion with Two-Phase Subsurface Reactions," *Journal of Propulsion and Power*, Vol. 11, No. 4, 1995, pp. 729–739.

[9]Kichin, Yu. S., and Bakhman, N. N., "Effect of a Molten Layer on the Surface of the Charge on the Initial Temperature Dependence of the Burning Rate," *Combustion Explosions and Shock Waves*, Vol. 6, No. 4, 1970, pp. 370–373.

[10]Egorshev, V. Yu., Kondrikov, B. N., and Yakovleva, O. I., "Combustion of Water-Impregnated Explosive Compounds," *Combustion Explosions and Shock Waves*, Vol. 27, No. 5, 1992, pp. 565–572.

[11]DeLuca, L. T., Cozzi, F., Germiniasi, G., Ley, I., and Zenin, A. A., "Combustion Mechanism of an RDX-Based Composite Propellant," *Combustion and Flame*, Vol. 118, 1999, pp. 248–261.

[12]Parr, R. G., and Crawford, B. L., Jr., "A Physical Theory of Burning of Double-Base Rocket Propellants: 1," *Journal of Physical and Colloid Chemistry*, Vol. 54, No. 6, 1950, pp. 929–954.

[13]Zanotti, C., Volpi, A., Bianchessi, M., and DeLuca, L. T., "Measuring Thermodynamic Properties of Burning Propellants," *Nonsteady Burning and Combustion Stability of Solid Propellants*, edited by L. T. DeLuca, E. W. Price, and M. Summerfield, Progress in Astronautics and Aeronautics, AIAA, Washington, DC, 1992, pp. 145–196.

[14]Zeldovich, Ya. B., "On the Combustion Theory of Powder and Explosives," *Journal of Experimental and Theoretical Physics*, Vol. 12, No. 11, 12, 1942, pp. 498–510.

[15]Zeldovich, Ya. B., Leypunskii, O. I., and Librovich, V. B., *The Theory of the Unsteady Combustion of Powder*, Nauka, Moscow, 1975, Chap. 8.

[16]Novozhilov, B. V., "Stability Criterion for Steady-State Burning of Powders," *Journal of Applied Mechanics and Technical Physics*, Vol. 6, No. 4, 1965, pp. 157–160.

[17]Novozhilov, B. V., "Burning of a Powder Under Harmonically Varying Pressure," *Journal of Applied Mechanics and Technical Physics*, Vol. 6, No. 6, 1965, pp. 141–144.

[18]Novozhilov, B. V., *Nonstationary Combustion of Solid Rocket Fuels*, Nauka, Moscow, 1973, Chap. 3 (Translation AFSC FTD-MT-24-317-74).

[19]Novozhilov, B. V., "Theory of Nonsteady Burning and Combustion Stability of Solid Propellants by the ZN Method," *Nonsteady Burning and Combustion Stability of Solid Propellants*, edited by L. T. DeLuca, E. W. Price, and M. Summerfield, Progress in Astronautics and Aeronautics, AIAA, Washington, DC, 1992, pp. 601–641.

[20]Denison, M. R., and Baum, E., "A Simplified Model of Unstable Burning in Solid Propellants," *ARS Journal*, Vol. 31, 1961, pp. 1112–1122.

[21]Krier, H., T'ien, J. S., Sirignano, W. A., and Summerfield, M., "Nonsteady Burning Phenomena of Solid Propellants: Theory and Experiments," *AIAA Journal*, Vol. 6, No. 2, 1968, pp. 278–288.

[22]Culick, F. E. C., "Calculation of the Admittance Function for a Burning Surface," *Astronautica Acta*, Vol. 13, No. 3, 1967, pp. 221–237.

[23]Culick, F. E. C., "A Review of Calculations for Unsteady Burning of a Solid Propellant," *AIAA Journal*, Vol. 6. No. 12, 1968, pp. 2241–2255.

[24]Culick, F. E. C., "Some Problems in the Unsteady Burning of Solid Propellants," U.S. Naval Weapons Center, TR NWC TP-4668, China Lake, CA, Feb. 1969.

[25]Lengellé, G., Kuentzmann, P., and Rendolet, C., "Response of a Solid Propellant to Pressure Oscillations," AIAA Paper 74-1209, Oct. 1974.

[26]Kumar, R. N., "Condensed Phase Details in the Time-Independent Combustion of AP/Composite Propellants," *Combustion Science and Technology*, Vol. 8, No. 2, 1973, pp. 133–148.

[27]Kumar, R. N., and Culick, F. E. C., "Role of Condensed Phase Details in the Oscillatory Combustion of Composite Propellants," *Combustion Science and Technology*, Vol. 15, No. 2, 1977, pp. 179–199.

[28]Lengellé, G., Bizot, A., Duterque, J., and Trubert, J. F., "Steady-State Burning of Homogeneous Propellants," *Fundamentals of Solid Propellant Combustion*, edited by K. K. Kuo and M. Summerfield, Progress in Astronautics and Aeronautics, AIAA, Washington, DC, 1984, pp. 361–407.

[29]Zarko, V. E., Gusacenko, L. K., and Rychkov, A. D., "Effect of Melting on Stability of Stationary and Transient Combustion Regimes of Energetic Materials," Workshop on Combustion Instability of Solid Propellants and Rocket Motors, Politecnico di Milano, Paper 97-06-02, June 1997.

[30]Louwers, J., and Gadiot, G. M. H. J. L., "Nonlinear Transient Burning of Composite Propellants: The Effect of Solid Phase Reactions," *Proceedings of Fourth International Symposium on Special Topics in Chemical Propulsion: "Challenges in Propellants and Combustion 100 Years After Nobel,"* edited by K. K. Kuo, Stockholm, July 1997, pp. 1146–1156.

[31]DeLuca, L. T., DiSilvestro, R., and Cozzi, F., "Intrinsic Combustion Instability of Solid Energetic Materials," *Journal of Propulsion and Power*, Vol. 11, No. 4, 1995, pp. 804–815; see also Comments, *Journal of Propulsion and Power*, Vol. 13, No. 3, 1997, pp. 454–456.

[32]DeLuca, L. T., "Radiation-Driven Steady Pyrolysis of Energetic Solid Materials," California Inst. of Technology, Karman Lab. of Fluid Mechanics and Jet Propulsion, TR CI97-3, Pasadena, CA, Aug. 1997.

[33]Pagani, C. D., and Verri, M., "Stability Analysis of the Travelling Wave Solutions in Burning Solid Propellants," *Proceedings of the First World Congress of Nonlinear Analysts*, edited by V. Lakshmikantham, de Gruyter, Berlin/New York, 1996, pp. 661–666.

[34]Son, S. F., and Brewster, M. Q., "Linear Burning Rate Dynamics of Solids Subjected to Pressure or External Radiant Flux Oscillations," *Journal of Propulsion and Power*, Vol. 9, No. 2, 1993, pp. 222–232.

[35]Hart, R. W., Farrell, R. A., and Cantrell, R. H., "Theoretical Study of a Solid Propellant Having a Homogeneous Surface Reaction: 1. Acoustic Response, Low and Intermediate Frequencies," *Combustion and Flame*, Vol. 10, No. 4, 1966, pp. 367–380.

[36]Brown, R. S., and Muzzy, R. J., "Linear and Nonlinear Pressure Coupled Combustion Instability of Solid Propellants," *AIAA Journal*, Vol. 8, No. 8, 1970, pp. 1492–1500.

[37]Beckstead, M. W., and Culick, F. E. C., "A Comparison of Analysis and Experiment for Solid Propellant Combustion Instability," *AIAA Journal*, Vol. 9, No. 1, 1971, pp. 147–154.

[38]T'ien, J. S., "Theoretical Analysis of Combustion Instability," *Fundamentals of Solid Propellant Combustion*, edited by K. K. Kuo and M. Summerfield, Progress in Astronautics and Aeronautics, AIAA, Washington, DC, 1984, pp. 791–840.

[39]Brewster, M. Q., and Son, S. F., "Quasi-Steady Combustion Modeling of Homogeneous Solid Propellants," *Combustion and Flame*, Vol. 103, No. 1–2, 1995, pp. 11–26.

[40]Kubota, N., "Temperature Sensitivity of Solid Propellants and Affecting Factors: Experimental Results," *Nonsteady Burning and Combustion Stability of Solid Propellants*, edited by L. DeLuca, E. W. Price, and M. Summerfield, Progress in Astronautics and Aeronautics, AIAA, Washington, DC, 1992, pp. 111–143.

[41]Boggs, T. L., Atwood, A. I., Curran, P. O., Parr, T. P., Hanson-Parr, D., and Paull, D., "The Pressure and Temperature Sensitivity of Burn Rates of Solid Propellant Ingredients," *International Symposium on Energetic Materials*, Xiangfan, Hubei, China, Sept. 1995.

[42]Atwood, A. I., Boggs, T. L., Curran, P. O., Parr, T. P., and Hanson-Parr, D., "Burn Rate Temperature and Pressure Sensitivity of Solid Propellant Ingredients," Politecnico di Milano, Paper 97-03-01, June 1997.